

A STUDY OF COMBINED EFFECTS OF ROTATION AND ADVERSE PRESSURE GRADIENT ON TURBULENT BOUNDARY LAYER FLOWS : PART 1 - MEAN FLOW RESULTS

G. IBAL¹ and P.N. JOUBERT²

¹Aeronautical Research Laboratory, DSTO, PO Box 1500, Salisbury, SA 5108, AUSTRALIA

²Dept Mechanical & Manufacturing Engineering, University of Melbourne, Parkville, VIC 3052, AUSTRALIA

1. ABSTRACT

The combined effects of rotation and adverse pressure gradient on turbulent boundary layer flows in a rotating plane wall diffuser are investigated. The mean flow, broadband-turbulence and spectral measurements are taken at a number of stations in both pressure and suction side layers for two different adverse pressure gradient distribution with different rotation rates. The mean flow results indicates the formation of a boundary layer separation on the suction (trailing) side of the diffuser, at stronger pressure gradient. The separated region developed after the separation is steady and relatively quiescent. Taylor-Gortler type vortices are observed on the pressure (leading) side wall.

2. NOMENCLATURE

C_E	: Entrainment rate
C_p	: Pressure coefficient
C_f	: Skin friction coefficient
C_{fm}	: Mean value of C_f in spanwise direction
H	: Shape parameter
h	: Diffuser inlet height
l	: Mixing length
R_θ	: Momentum thickness Reynolds number
$R_{r,f}$: Unit Reynolds number based on U_e at inlet and W
Ri	: Richardson number, $Ri=S(S+1)$ as $S=-2\Omega/(\partial U/\partial y)$
st-i	: Measurement station, $i=1,4$
U	: Mean velocity in streamwise direction (x direction)
U_e	: Free stream velocity at the edge of boundary layer
W	: Diffuser inlet width
δ	: Boundary layer thickness
θ	: Boundary layer momentum thickness
Ω	: Rotation speed (rad/s, anticlockwise positive)

3. INTRODUCTION

A set of experiments have been performed in the rotating wind tunnel of Melbourne University. The motivation for the present experiments has been to obtain a better understanding of complex turbulent flows which are defined by Bradshaw (1973) as "shear layers with complicating influences like distortion by extra rates of strain or interaction with another turbulence field". These extra strain rates can be named as longitudinal curvature, system rotation, bulk compression or dilatation, lateral

straining, etc. The current study was intended to investigate the combined effects of rotation and adverse pressure gradient, leading to two extra components, which are equal to Ω and $\partial U/\partial x$ respectively, in addition to the simple shear $\partial U/\partial y$.

A turbulent boundary layer in a rotating diffuser is known to be a good example of the above complex flows. As the diffuser flows get more complicated in structure (for example those with system rotation, longitudinal vortices, corner flows or separated regions), the existing prediction methods become less capable of calculating them. This is in part due to a lack of understanding of the physics which must come from experiments. According to the literature survey given by Ibal (1990), no complete experimental data is yet available for the above type of complex flows.

Therefore, the aims of the current investigation can be summarized as;

(i) to obtain a large set of experimental data for the case of adverse pressure gradient and separating turbulent boundary layer flows with system rotation,

(ii) to determine the empirical constants which can be used in prediction methods for the relevant flow cases, and thus gain a better understanding of turbulence structure of these types of complex flows.

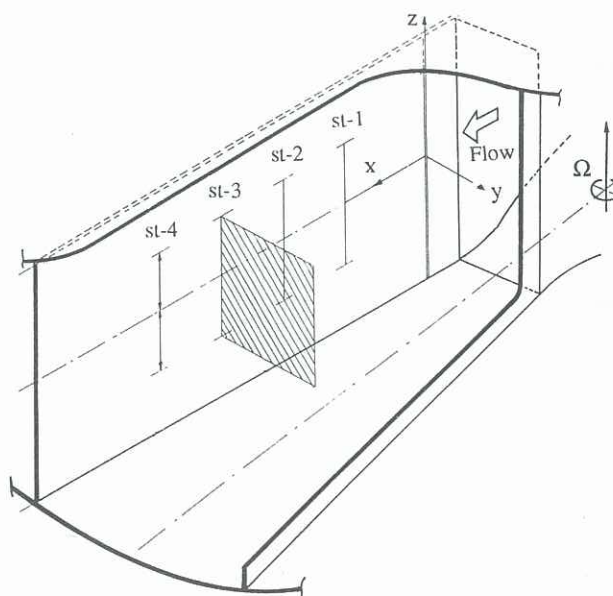


Fig 1. Isometric sketch of the working section.

¹ Postal Address: Aeronautical Research Laboratories, DSTO, GWD, Salisbury, PO 1500, SA 5108, Australia.

4. EXPERIMENTAL PROGRAM

Measurements are presented for low-Reynolds-number turbulent boundary layers developing in adverse pressure gradients on the side walls of a rotating plane-wall diffuser with variable area ratio. Diffuser had cross-sectional dimensions of 600mm (h) and 156mm (W) at the inlet and was 1800mm long. The opening angles were 3 and 8 degrees for case 1 and 2 respectively (see Ibal, 1990). The entry laminar boundary layers were tripped with a 1mm diameter tip wire which was located at the origin of the coordinate system used (see fig 1). The free stream turbulence intensity was kept below 0.25% for all flow cases. A large number of hot wire measurements were taken

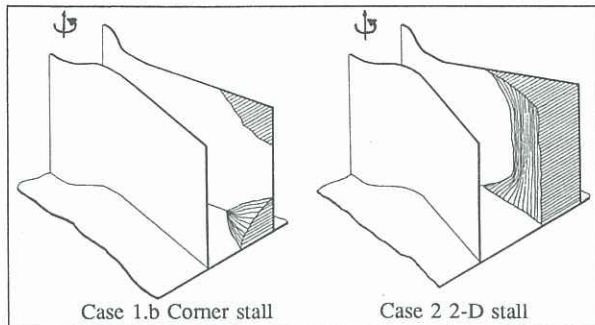


Fig 2. Typical stall patterns in the present experiments.

in the turbulent boundary layers developing on the side walls of the diffuser, at a specified unit Reynolds number, $R_{\tau}=664000$, which corresponded an inlet reference velocity of 10 m/s (U_c).

Hot wire signals were extracted from the apparatus via a slip ring and brush assembly which also provides access for power and control signals. Hot wire signals were passed through Krohn-Hite low-pass filters. The filters were set at a roll-off frequency of 30 Hz for dynamic calibration (see Perry, 1982). The roll-off frequency of the filters were set to be 10 kHz for the turbulence measurements. All signals were sampled by a PDP 11/10 digital computer using a 12 bit analogue-to-digital convertor. Sampling was in bursts of 8000 samples while the sampling frequency was 200 Hz. The validity of the single and crossed hot wire measurements near separation was checked using the criteria given by Nagabushana et al (1988).

Pressures were measured with a differential electronic manometer mounted on the tunnel. Wall distances were determined from the traverse display which was initially set after finding the point where the probe was just leaving the wall.

5. OBSERVATIONS & CONCLUDING REMARKS

Three two-dimensional, low Reynolds number, turbulent, adverse pressure gradient boundary layers developing on the side walls of a rotating-plane-wall diffuser have been investigated experimentally.

Case 1.a: Here turbulent boundary layers developing on the side walls of a rotating diffuser with opening angle of 3° and rotation rate of 40 rpm were studied. No apparent stall was observed in the diffuser.

Case 1.b: This case had the same adverse pressure gradient as Case 1.a, but a higher rotation rate (60 rpm). Pockets of corner stalls appeared at the top and bottom of the suction side wall.

Case 2: For this case, turbulent boundary layers developing on the side walls of a rotating diffuser with opening angle of 8° (which represents a stronger adverse pressure gradient than case 1) and rotation rate of 40 rpm were investigated. A steady two-dimensional stall on the suction side wall was observed at a streamwise distance of $x > 620$ mm (which is approximately 4 times the inlet width).

All stationary cases have been carefully checked for spanwise uniformity. Some of the features of the flow cases studied in the present investigation with concluding remarks are;

1) The turbulent boundary layers developing in the presence of adverse pressure gradients were found to be attached everywhere for the stationary cases. However, the same boundary layers separated at downstream stations of the suction side wall when the system rotated. Pockets of corner stall (case 1.b) and two-dimensional stall (case 2) appeared on the suction side wall of the rotating diffuser (see fig 2).

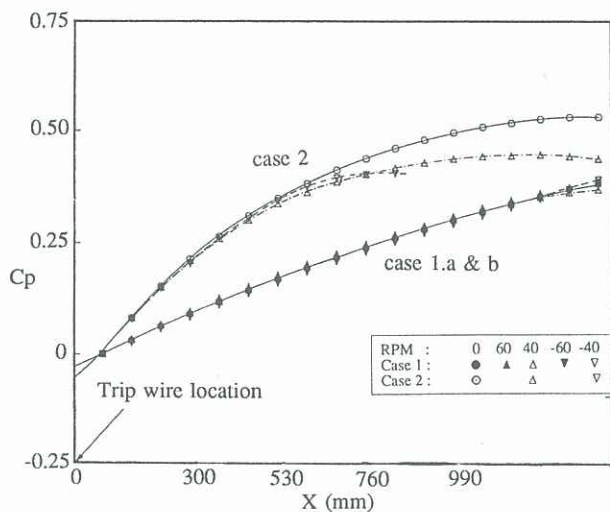


Fig 3. C_p values for case 1 and 2.

2) The turbulent boundary layer development and the general features of the flow patterns containing stall were altered by increasing both the rotation and the adverse pressure gradient.

3) The separated region developed after the two-dimensional separation was steady and relatively quiescent.

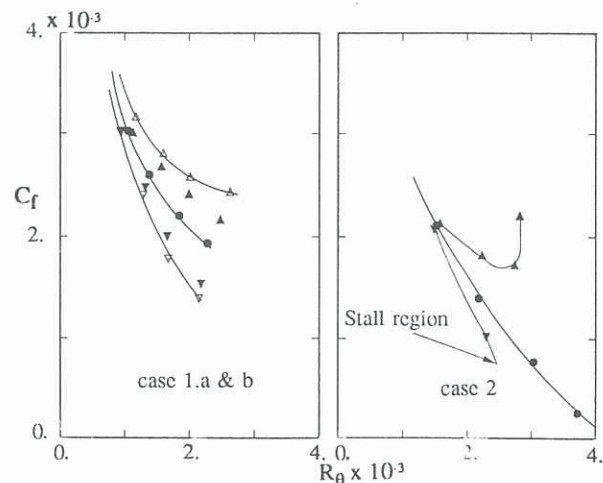


Fig 4. The development of skin friction coefficients with R_{θ} . Δ, \triangle ; 40 rpm, 60 rpm (pressure side), ∇, ∇ ; -40 rpm, -60 rpm (suction side), \bullet ; no rotation,

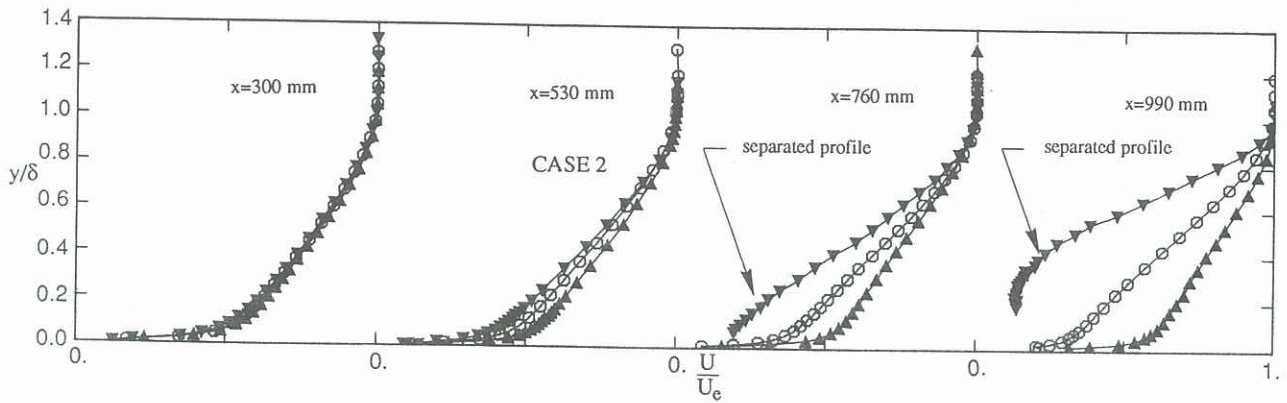


Fig 5. Mean velocity profiles for case 2. Note shift in abscissa.
 \circ ; stationary, Δ, \blacktriangle ; 60 rpm, 40 rpm (pressure side), $\nabla, \blacktriangledown$; -60 rpm, -40 rpm (suction side).

4) When the flow was in the corner stall regime, case 1.b, a steady pressure rise in the streamwise direction was observed indicating that the flow continued to diffuse (see fig 3). However, for two-dimensional stall regime for case 2, the pressure recovery was found to be reduced in the rotating layers as compared to the non-rotating layer. It appears that the flow stopped diffusing after the region where the flow separation occurred.

5) Considering the C_f distribution in the streamwise direction, a significant decreasing trend in C_f values was observed as the opening angle of the diffuser was increased (increase in adverse pressure gradient). Introduction of rotation to the above diffuser flow caused the values of the skin friction coefficients to be higher/lower in the pressure/suction side boundary layer as compared to the non-rotating boundary layer (see fig 4). The deviation of C_f values from the case of zero rotation was found to be proportional to the rotation rate, except in the region where the stall occurred.

6) Velocity gradients near the wall were

reduced/increased in the suction/pressure side layers as compared to those in the non-rotating layers (see fig 5). Increasing opening angle caused a reduction in the near wall velocity gradients of both side walls of the rotating diffuser.

7) Shape parameters, (H) , were higher/lower in the suction/pressure side layers as compared to those in the non-rotating layers, altered as a function of rotation rate.

8) Momentum thickness (θ) , momentum thickness Reynolds number, (R_θ) and boundary layer thickness (δ) were found to be mildly suppressed/enhanced in the suction/pressure side layers as compared to non-rotating layers. In the regions where the separation occurred, the values of above parameters on the pressure side wall appeared to be reduced due to the flow deflection effects caused by the flow separation on the suction side.

9) In the spanwise direction, large spatially periodic spanwise variation of C_f were observed for each flow case as an indication of Taylor-Gortler like vortices (roll cells) on the pressure side wall (see fig 6 and 7). Considering the

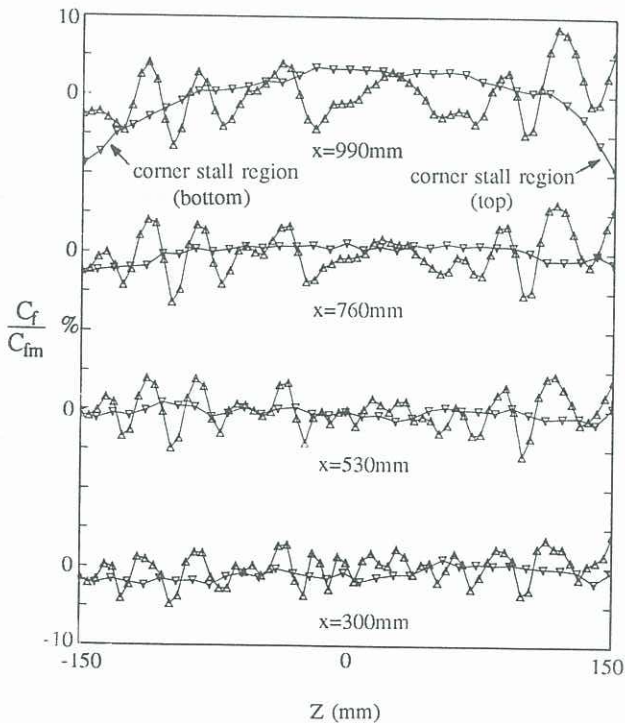


Fig 6. C_f/C_{fm} variation in spanwise direction. Note shift in ordinate.
 Case 1.b, Δ ; 60 rpm (pressure side), ∇ ; -60 rpm (suction side).

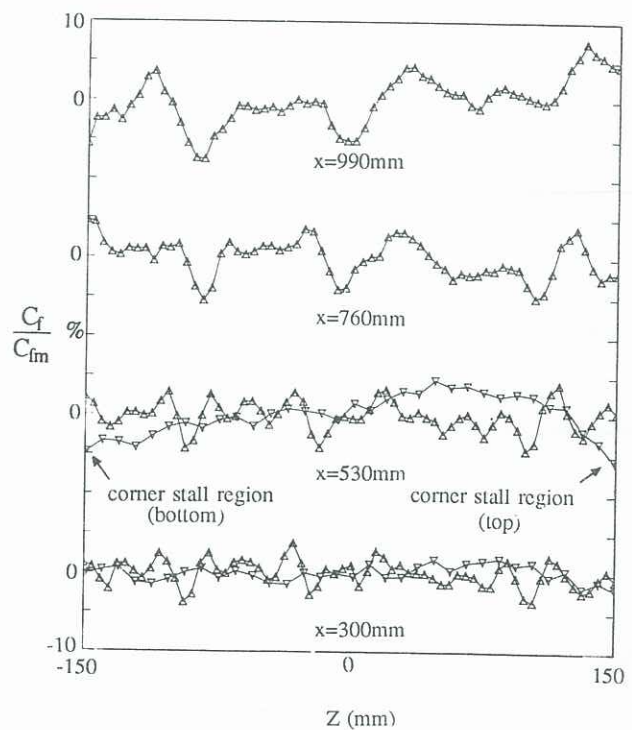


Fig 7. C_f/C_{fm} variation in spanwise direction. Note shift in ordinate.
 Case 2, Δ ; 40 rpm (pressure side), ∇ ; -40 rpm (suction side).

separated flow case, case 2, the wavelength of these variations did not remain constant and increased in streamwise direction in contrast with the findings of Tani (1962) and Watmuff et al (1985). It is most likely that the flow deflection effects, caused by the boundary layer separation on the suction side, creates significant changes in the roll cells patterns on the pressure side wall (fig 7). This might be the reason why the wavelength of these variations increased at downstream region for case 2. No measurement was taken further downstream because of the limits of the travers mechanism. Therefore, an open question remains: will these vortices disappear in the further downstream regions where the deflected flow effects are more strong?. No apparent periodic variation was measured on the suction side wall. However, a decreasing trend in the C_f values was found in the regions close to the top and bottom walls of the suction side as an indication of pockets of corner stall.

10) Richardson number (Ri) was employed as a local stability parameter of the flow and it was found that increasing rotation rate made the flow more stabilized/destabilized on the suction/pressure side (see fig 8.a). The same effect was observed when we compare Ri values of rotating layers for different diffuser opening angles (see fig 8.b). The flow was more stabilized/destabilized on the suction/pressure side for case 2 as compared to case 1.a. It was also appeared that increasing diffuser opening angle affected the local stability mainly in the inner layer while increasing rotation rate affected the whole layer.

11) Entrainment rate, C_E , was increased/decreased in the pressure side layers as compared to the non-rotating layers.

12) Mixing length, l , is known to be a measure of turbulent activity in a given velocity gradient. It was found that mixing length was increased/decreased in the

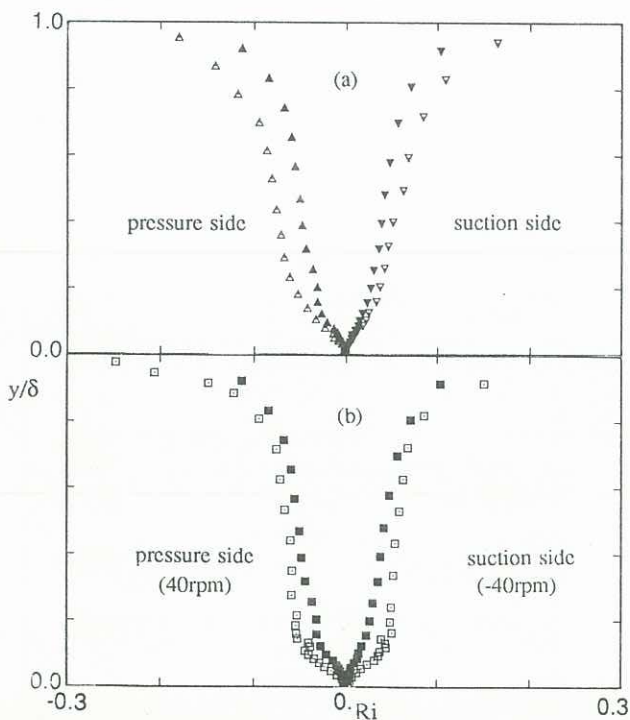


Fig 8. Variations of Ri at x=530 mm.
a) with rotation rate. Δ, \blacktriangle : 60, 40 rpm (pressure side),
 $\nabla, \blacktriangledown$: -60, -40 rpm (suction side), for case 1,
b) with opening angle, \blacksquare : case 1, \square : case 2.

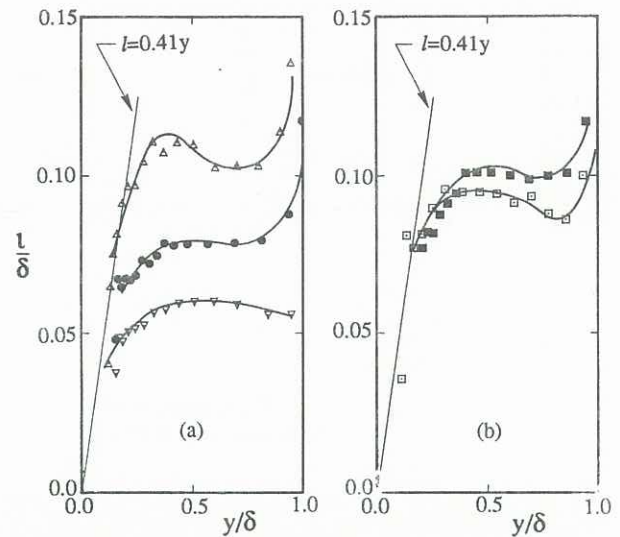


Fig 9. Profiles of mixing length.
a) profiles at x=990mm for case 1,
 \bullet : no-rotation, Δ : 60rpm (pressure side), ∇ : -60rpm (suction side)
b) pressure side profiles (40rpm) at x=530mm. \blacksquare : case 1, \square : case 2.

pressure/suction side layers as compared to those in the non-rotating layers (see fig 9.a). Increasing diffuser opening angle decreased the mixing length values significantly on both side walls (see fig 9.b).

6. REFERENCES

- BRADSHAW, P 1973 Effects of streamline curvature on turbulent flow. AGARD Dograph 196.
IBAL, G 1990 Adverse pressure gradient and separating turbulent boundary layer flows with system rotation. Ph.D Thesis, The University of Melbourne.
PERRY, A E 1982 Hot-wire anemometry. Oxford University Press, New York.
TANI, I 1962 Production of longitudinal vortices in the boundary layer along a concave wall. J. Geophys. Res. **67**, 3075-3080.
NAGABUSHANA, K A, AGARWAL, N K & SIMPSON, R L 1988 Features of separating turbulent boundary layers. AIAA-88-0616.
WATMUFF, J H, WITT, H T & JOUBERT, P N 1985 Developing turbulent boundary layers with system rotation. J. Fluid Mech. **157**, 405.